Structural Engineering and Mechanics, *Vol. 59, No. 6 (2016) 1055-1070*
DOI: http://dx.doi.org/10.12989/sem.2016.59.6.1055

Free vibration and buckling analysis of the impacted hybrid composite beams

Emin Ergun[1], Yasin Yilmaz[1] and Hasan Çallioğlu*[2]

[1]*Mechanical Engineering Department, Pamukkale University, Denizli, 20070, Turkey*
[2]*Automotive Engineering Department, Pamukkale University, Denizli, 20070, Turkey*

(Received January 28, 2016, Revised March 28, 2016, Accepted May 11, 2016)

Abstract. The aim of this experimental study is to investigate the free vibration and buckling behaviors of hybrid composite beams having different span lengths and orientation angles subjected to different impact energy levels. The impact energies are applied in range from 10 J to 30 J. Free vibration and buckling behaviors of intact and impacted hybrid composite beams are compared with each other for different span lengths, orientation angles and impact levels. In free vibration analysis, the first three modes of hybrid beams are considered and natural frequencies are normalized. It is seen that first and second modes are mostly affected with increasing impact energy level. Also, the fundamental natural frequency is mostly affected with the usage of mold that have 40 mm span length (SP40). Moreover, as the impact energy increases, the normalized critical buckling loads decrease gradually for 0° and 30° oriented hybrid beams but they fluctuate for the other beams.

Keywords: hybrid composites; vibration; buckling; impact behaviour; damage mechanism

1. Introduction

In the design of the structural components, it is necessary to go beyond the selection of materials with the appropriate properties. Developing hybrid composite structures can be effective in solving some of the critical and rugged engineering problems. Hybrid composites are composites in which two different types of fibers are combined. Popular hybrid fibers are glass and carbon fibers. By adding hybrid fibers to aramid fiber composites, several improvements can be achieved (Pandya *et al*. 2011, Sevkat *et al*. 2010, Wu *et al*. 2010). Over the past decade, fiber-reinforced polymers and variety of hybrid composites have been extensively used in various industries such as aerospace, marine, transportation and defense, because of their high specific strength, stiffness, long performance life and low maintenance properties.

Impact is one of the dangerous failure types for structural components, especially at low velocities, because the delamination damage may not be seen by visual inspection. Significant damages in composites, such as matrix cracks and delamination occur after the impact. Impact-based delamination causes manifestly reduction in stiffness, strength, and stability of the hybrid composite beams and plates. Hence, impact event is very important in design.

*Corresponding author, Associate Professor, E-mail: hcallioglu@pau.edu.tr

http://www.techno-press.org/?journal=sem&subpage=8 ISSN: 1225-4568 (Print), 1598-6217 (Online)

There are many studies on the impact response and damage mechanism of the composite structures for the last two decade. The impact force, the absorbed energy and the damaged area of the composite materials is investigated according to different energy levels and stacking sequences by Onal and Adanur (2002), Gideon *et al*. (2015). Compression or bending after impact tests (CAI and BAI) are used to get the retain strength of composite materials. Naik *et al*. (2002) carried out the compression after impact tests for impacted specimens using NASA fixture. Results showed that damage tolerance was higher for low mass and high velocity combination as compared to high mass and low velocity combination. Saeed *et al*. (2014) investigated the effects of impact and drilling damage types on compression strength of woven carbon-fiber/epoxy composites. After the three different tests applied, they mentioned that impact damage on the compression strength of the composites has more hazardous effect than drilling. Also, they said that damage mechanisms (interlaminar shearing, constituent microcracking), and longitudinal splitting played important role in the propagation of initial cracks/microcracks due to impact and drilling.

One of the ways to improve the impact resistance of composite materials is hybrid technology. The combining of different types of fibers into a single matrix has led to the development of hybrid composites (Swolfs *et al*. 2013, Fiore *et al*. 2011). It is generally known that the properties of hybrid composites can be controlled by some parameters such as matrix, fiber, fiber-matrix interface and hybrid design, etc. (Mishra *et al*. 2003, Siddeswarappa and Mohamed 2009). Nevertheless, the impact properties of the hybrid composites have not been studied extensively. Some of these: Davoodi *et al*. (2012) focused on improving the impact property of hybrid kenaf/glass fibre epoxy composite. They developed a hybrid composite to use in the car structural parts with geometrical improvement for an improvement of impact resistance of the bumper beam. Ghasemnejad *et al*. (2013) investigated damage behaviors of natural stitched composite single lap-joints under low velocity impact loading conditions. They applied charpy impact test to study the energy absorbing capability of single lap hybrid composite joints. Sayer *et al*. (2010) studied experimentally the impact responses of two different hybrid composite laminates and two different stacking sequences. They inspected visually the damaged specimens under various impact energies and used for comparison and identifying damage mechanisms. Gustin *et al*. (2005) conducted compression after impact tests on carbon fiber and Kevlar combination sandwich composites to determine the reduction in compressive strength for impacted and non-impacted specimens. Petrucci *et al*. (2015) investigated the impact and flexural post-impact behaviour of hybrid composites. The ternary hybrid composites (FHB, GHB and GFB) were composed of with different types of fibers, basalt (B), flax (F), hemp (H) and glass (G) with epoxy resin. As comparison of their impact performances, it was found to FHB appeared to be slightly overperforms than GFB whereas GHB was the worst performing hybrid laminate.

Looking at the literature, it is seen that free vibration and buckling analyses of impacted hybrid composites are rather limited although there are much more study on free vibration analysis of general laminated composites. Velmurugan and Balaganesan (2011) investigated the effect of nano clay incorporation in the epoxy/glass fiber laminates subjected to medium velocity of impact. Frieden *et al*. (2011) studied the change of natural frequencies of carbon fiber reinforced polymer plates due to low energy impact damage and they showed that the damaged area could change eigenfrequency of the composites. Kiral *et al*. (2012) presented the effect of impact failure on the natural frequency and the damping ratio of the cantilever woven-epoxy composite beams using the envelope curve and the logarithmic decrement. Zor *et al*. (2004) investigated the effects of the strip vertical or horizontal delamination width on the buckling loads of laminated composite plates by using three-dimensional finite element models. The results in that study show that important decrease in the buckling loads occurs after a certain value of the delamination width. Tercan and Aktas (2009) studied the cutout shape effects on the buckling behavior of rib knitting glass/epoxy laminated plates in three different knitting tightness levels as low, medium and high. Their results are showed that the buckling loads depend on the cutout area and the level of tightness. Ergun (2010) investigated the change in the critical buckling load due to different composite lamina numbers, orientation angles, stacking sequences, boundary conditions as a function of temperature, experimentally and numerically. Çallioglu and Ergun (2014) dealt with the effects of the different impact points, energy levels, and thickness on the buckling behaviors of the impacted composite plates. They said that the lowest critical buckling load occurred in thin plates impacted at the center point and the critical buckling loads becomed more stable in the other impact points.

In the present work, the hybrid composite beams having three different span lengths, (40, 60 and 80 mm), are first impacted at different energy levels, (10, 20 and 30 J). After the impact test, the free vibration (modes 1, 2 and 3) and buckling behavior of the impacted hybrid composite beams are determined. Free vibration and buckling behaviors of impacted and non-impacted hybrid composite beams are compared with each other for different span lengths, orientation angles and impact levels.

2. Production of composite beams

In this work, the hybrid composites plates are manufactured from E-glass (200 gr/m^2) and Carbon woven fabrics (245 gr/m^2) and epoxy resin by using vacuum assisted resin infusion method (VARIM). The production is implemented on a vacuum device and control unit connected to a heater table. A matrix based on Huntsman Araldite LY-1564 epoxy and Aradur 3487 hardener is used in the manufacture of the hybrid composite plates. The weight mixing ratio for resin-to-hardener is about 100:34, and the total fiber and matrix volume fraction of the plate is calculated as 50 %.

The hybrid composite plates are cured with the heater plate, at a constant 2 atm vacuum pressure and at 60°C temperature for 2 hours. Then, the hybrid composite plates are cooled down to the room temperature maintaining the pressure. Thickness of the composite plates is approximately measured 3.2 mm after the process of trimming. The orientation angles used in hybrid composite plates with 16 plies are $(C_0/G_0/(C_0/G_0)_3)_s$, $(C_0/G_0/(C_{15}/G_{15})_3)_s$, $(C_0/G_0/(C_{30}/G_{30})_3)_s$ and $(C_0/G_0/(C_{45}/G_{45})_3)_s$ and in this study, they are represented by CG0, CG15, CG30 and CG45, respectively. Here, C and G represent carbon and glass fibers, respectively. After manufacturing process, the beam specimens to be used in the experiments are cut from the hybrid composite plates in dimensions of 40×260 mm by water jet.

3. Experimental procedures

3.1 Impact test

The hybrid composite beam specimens are subjected to the impact tests by using Instron®-Dynatup® 9250 HV model instrumented drop weight impact testing machine. The testing machine records and accumulates the impact parameters, such as height, velocity and energy. The impactor of the testing machine has a 12.5 mm diameter hemispherical tip. The total mass of the impactor is

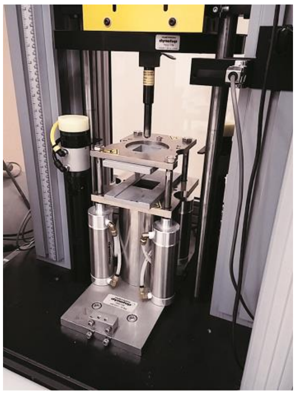

Fig. 1 The impact testing machine with the attached mold

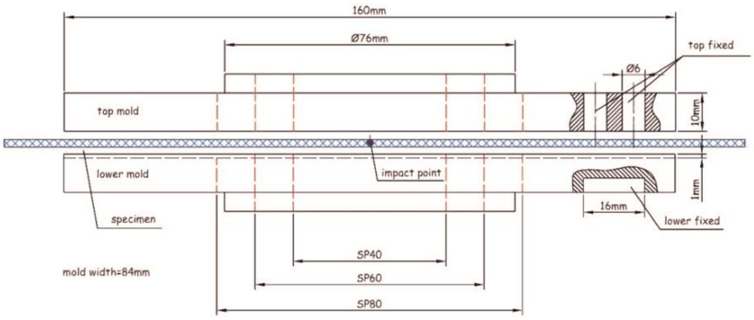

Fig. 2 Schematic representation and dimensions of a composite beam

approximately 6.32 kg.

The beam specimens were clamped with the three different rectangular molds, which were attached to the pneumatic fixture of the machine, in order to determine the effects of span lengths on the bending rigidities of the beams during the impact event. The mold that is used to fix hybrid composite beams and impact testing machine are shown in Fig. 1.

The cross-sectional channel profiles of the three different rectangular molds were chosen as SP40 (40 mm×40 mm), SP60 (60 mm×40 mm) and SP80 (80 mm×40 mm). SP symbol represents the longitudinal span in the molds. A schematic representation and dimensions of a hybrid composite beam between the molds is given in Fig. 2. The hybrid composite beams were impacted at three different impact energy levels of 10, 20 and 30 J at their center. All the tests were approximately carried out at the room temperature of 23℃.

3.2 Vibration tests

Free vibration analyses were carried out using DEWESoft vibration measurement device DEWE43A (Dewesoft, Trbovlje, Slovenia). This instrument has eight analog inputs with 200 kS/s/ch maximum sampling rate and 24-bit AD converter. Modal analysis is essential part of a free vibration analysis. In the present study, impact hammer testing method is used for modal analyses. Beams are clamped at one end and other end is left free to vibrate. The effective length of the beam is 220 mm. An accelerometer is located at 20 mm away from free end of the beam. The

Fig. 3 The setup for free vibration analysis

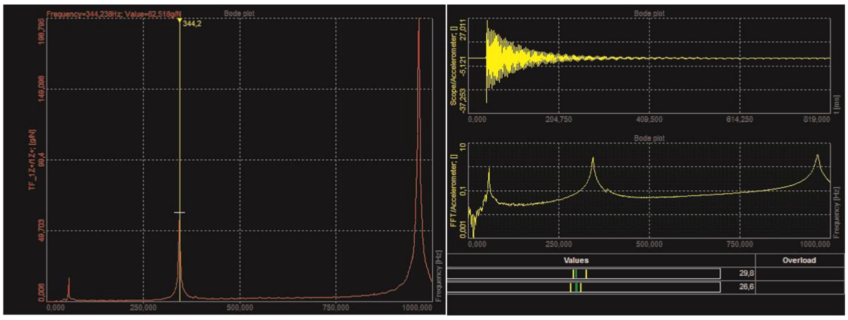

Fig. 4 Acceleration response and its frequency spectrum for the beam of type CG15 impacted at 10 J using mold with span length 80 mm

accelerometer used is the Dytran model 3224A1 (Dytran Instruments Inc., CA, USA) which is an ultra-miniature teardrop IEPE accelerometer with integral electronics. It has an overall weight of 0.2 g and a sensitivity of 10 mV/g. The beams were excited with the impulse hammer, Dytran model 5800SL (Dytran Instruments Inc., CA, USA). It is an IEPE impulse hammer with a measurement range of 50 lbf and has a mass of 9.8 g. It has a very high stiffness and a sensitivity of 100 mV/lbf. The vibration data taken from the vibration measurement device is sent to program DEWESoftX to calculate the first three natural frequencies of the beams. The setup is shown in Fig. 3.

In free vibration analyses, 10 specimens were used for each configuration, CG0, CG15, CG30 and CG45. Firstly, modal parameters of the intact composite beams are determined for each configuration and then nine beam specimens from each configuration are subjected to 3 different impact energy levels varying from 10 J to 30 J using three different molds having three different span lengths, 40 mm, 60 mm and 80 mm. The beams impacted at different energy levels are then subjected to vibration testing again and first three natural frequencies of them are determined. As an example, the acceleration response and its frequency spectrum for the beam configuration CG15 impacted at 10 J using mold SP80 mm is shown in Fig. 4.

3.3 Buckling tests

To determine the buckling behaviors of the intact and impacted hybrid composite specimens at different span lengths, orientation angles and energy levels, Instron 8801 Servo hydraulic testing machine with 50 kN loading capacity has been used, as seen in Fig. 5. Both ends of the specimen

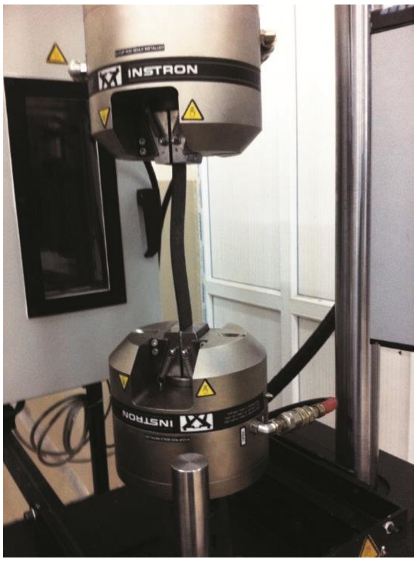

Fig. 5 Application of the buckling test to the specimens

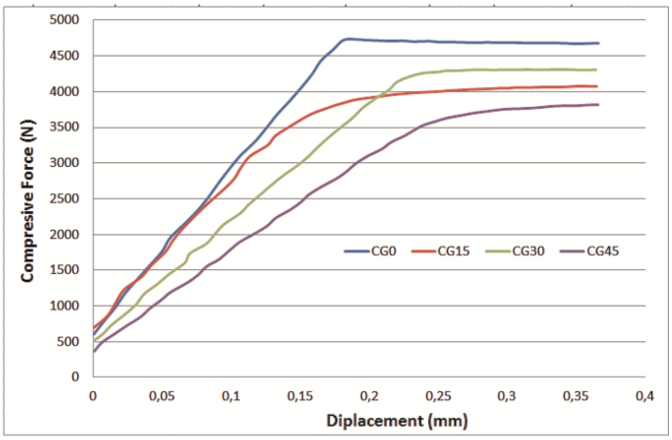

Fig. 6 Loads versus displacements curves

are clamped into the machine's jaws, one of which is movable toward and away from the other. Axial Servo hydraulic testing machine has an adjustable crosswise head and its maximum hydraulic pressure is 207 bars. The axial compression tests are performed using displacement control with a speed of 0.2 mm/min. During the test, the load versus displacement (contraction) curve is measured and recorded automatically by test machine. The hydraulic pressure in the head of machine during buckling tests was almost 38-40 bars. There is not observed any damage in the surface of the specimens subjected to this pressure and slip between the specimen and machine's jaws.

Buckling loads versus displacements are plotted in Fig. 6 for different orientation angles of the intact composite beams. Moreover, the critical buckling load (P_{cr}) can be determined from the same figure (Ergun 2010). The effective length of the beams for buckling analysis is taken to be 200 mm.

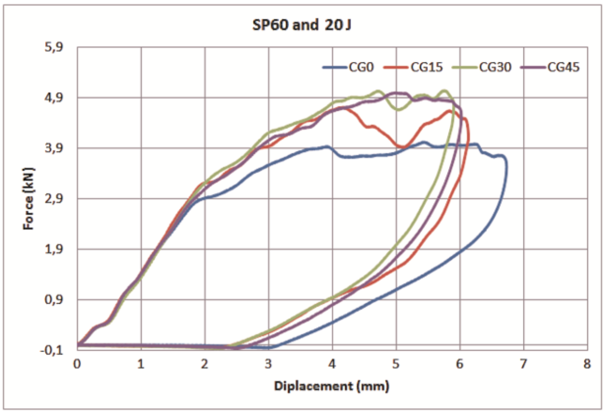

Fig. 7 Force versus displacement curves for SP60 configuration at 20 J

4. Results and discussion

To understand better the free vibration and buckling behaviors of the impacted hybrid composite beams, the hybrid composite beams having three different span lengths are first impacted at different energy levels with the impact testing machine (Instron Dynatup 9250 HV). After the impact test, to determine the free vibration and buckling behavior of the impacted hybrid beam specimens, modal analyses and buckling experiments are carried out. Impacted and non-impacted specimens are compared with each other to see the effects of span length, orientation angles and different impact energy levels on free vibration and buckling behaviors of hybrid composite beams.

4.1 Impact behavior of the hybrid composite beams

The important impact characteristics, such as the impact load, deflection, and contact time, yield the impact behaviors of the hybrid composite beams. It is known that the force-deflection (F-d) curve is a response to the impact loading of the hybrid composite beams and it gives significant information about the impact behavior of the hybrid beams during an impact event (Sayer *et al*. 2010). This curve is obtained from the contact of the impactor to the specimen. For comparison, force-deflection curves of the hybrid composite beams of SP60 with different orientation angles subjected to 20 J impact energy are given in Fig. 7. As seen in this figure, each curve has an ascending section of loading, reached a peak contact force value, and a descending section of unloading. When the impactor makes contact with the specimens, loading section of force-deflection curves increases for each composite. The ascending section of force-deflection curve occurs due to the resistance of hybrid composite to the impact loading. A plateau may occur in some contact force-deflection curves. The plateau represents reduction in stiffness of the hybrid composite specimens, implying there is more damage accumulation at the lower layers of the specimens. The descending section of load-deflection curves represents impactor rebounding from specimen surface.

Slope in ascending section of F-d curve represent the bending stiffness of the hybrid composite beams. Although all of the hybrid composite beams with the different orientation angles have firstly the same slope, the slope changes due to the different damage size in the hybrid composite

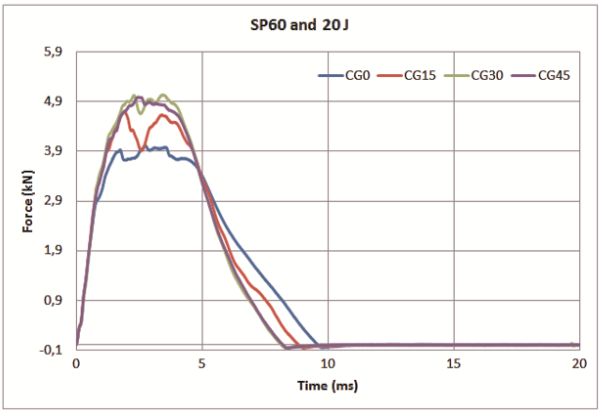

Fig. 8 The force versus time curves for SP60 configuration at 20 J

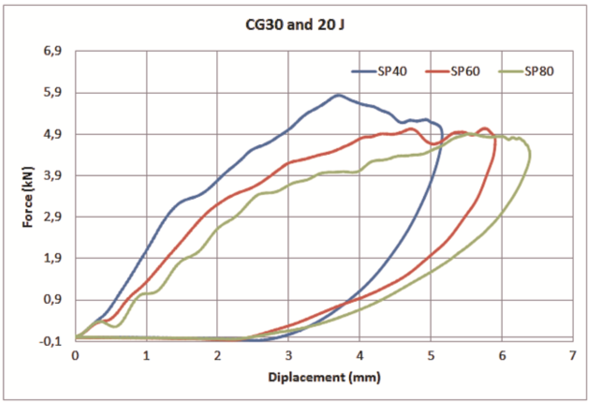

Fig. 9 Force versus displacement curves for CG30 beam at 20 J

beams with different angles. In the hybrid composite specimens subjected to impact, the penetration and perforation damages are not allowed in order to take the effects of small damage sizes on the buckling and vibration behaviors into consideration. Thus, F-d curves of all the hybrid composite beams are in the closed form at the applied impact energies.

The maximum peak force, 5 kN, occurs in CG30 and CG45 configurations, whereas minimum contact force, 4 kN, occurs for CG0 configuration. The permanent deflection of CG0 composite has a higher value, 3 mm, as compared with the other hybrid composites. The both maximum and permanent deflections, 6 mm and 2.45 mm respectively, of the other composite beams are approximately the same. A reduction in the plateau region of the contact force-deflection curve of the CG15 configuration take places due to unstable fiber breakage that occurs in inner layers of the composites.

The force versus contact duration between impactor and SP60 hybrid composite beams that have different orientation angles and subjected to 20 J impact energy is shown in Fig. 8. The contact times of CG30 and CG45 configurations are the same as well as their contact forces at this energy level. Although the contact force of CG0 composite is the lowest, its contact time is the largest due to the formation of the plateau section, as can be seen in its F-d curve. Nevertheless, although a force reduction in the upper region of F-d or F-t curves of CG15 composite due to the

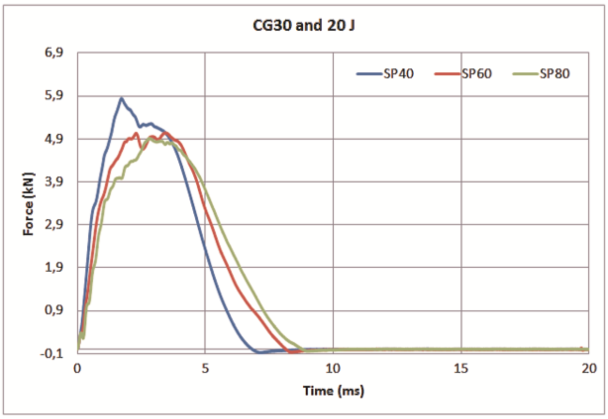

Fig. 10 Force versus time curves for CG30 beam at 20 J

fiber breakages occurs, its contact time value remains among others.

Fig. 9 shows F-d curve for CG30 hybrid composites having different span lengths under 20 J impact energy. As expected, the bending rigidity of the hybrid composite beams decreases gradually by increasing span length. Similarly, their peak forces also decrease. Unlike of this situation, as span length increases the displacement increases, the maximum displacement value is obtained for SP80 hybrid composite beam, which shows in this figure. However, the permanent displacement is the highest for the SP40 hybrid composite beam. The crack onset in resin of composites and damage can take place during impact testing. As the impact energy increases, the damage area increases. As a result of this, the bending rigidity of the composite beams decreases.

Fig. 10 depicts F-t curve for CG30 configuration having different span lengths under 20 J impact energy. The contact time increases with increasing span length. Therefore, the minimum contact time occurs in the hybrid composite beam of SP40, whereas the maximum contact time occurs in the hybrid composite of SP80.

4.2 Vibration behavior of the hybrid composites

Free vibration analyses are carried out on all beams before and after the impact tests. First, average values of first three natural frequencies of 10 beam specimens are calculated for the intact beams of all types and then natural frequencies of impacted beams are normalized using the following formula (Eq. (1))

$$\omega^* = \frac{\omega_{impacted\_beam}}{\omega_{intact\_beam}} \tag{1}$$

The variations of first three natural frequencies of beams with respect to impact energy induced on them are given in Figs. 11-13. In addition, the effect of span length on natural frequencies of the hybrid composite beams can also be seen from these figures.

From Fig. 11, it is seen that the first natural frequencies of all beam configurations (CG0, CG15, CG30 and CG45) are affected mostly with the usage mold with span length 40 mm in impact testing. This is due to the fact that in this situation the beams cannot bend easily until those of the other span lengths occur, and matrix cracking and fiber breakage increase. SP60 and SP80

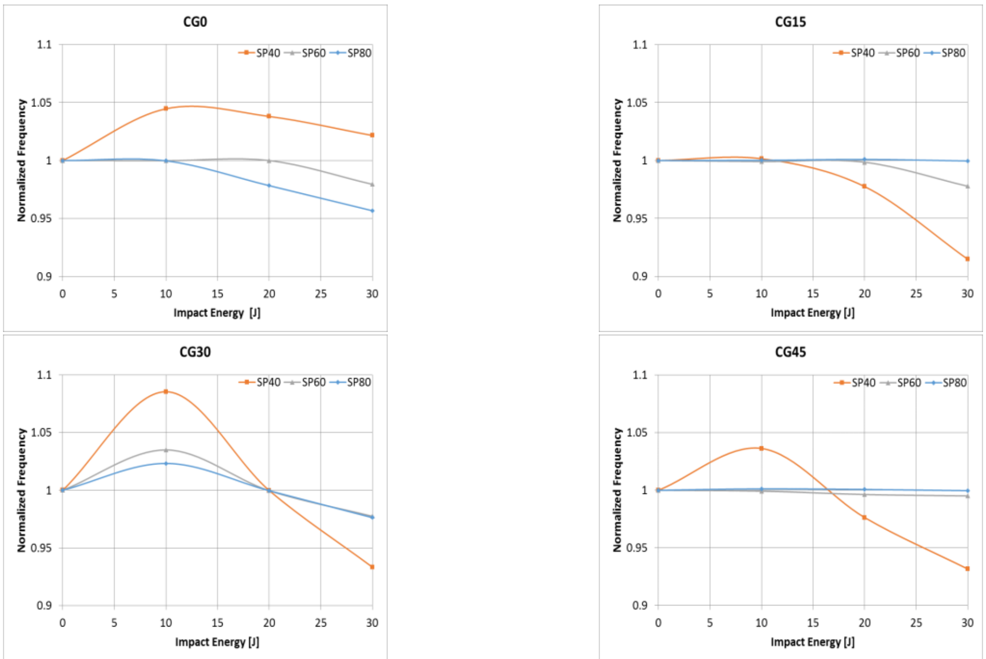

Fig. 11 Variation of first natural frequency of beams with impact energy induced on them

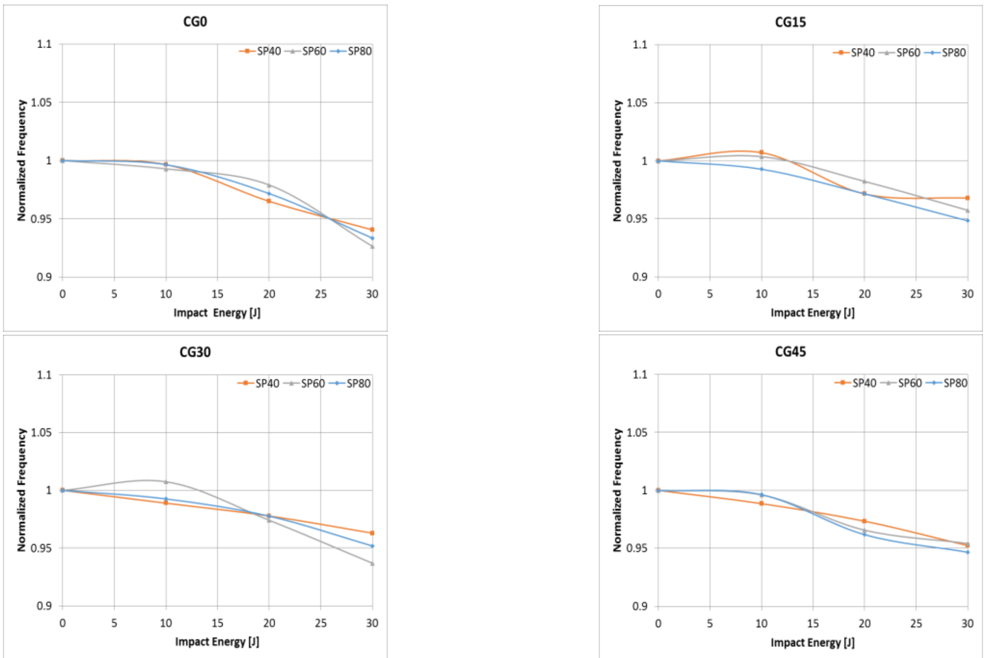

Fig. 12 Variation of second natural frequency of beams with impact energy induced on them

hybrid composite beams nearly show same trend. At low impact energy levels, an increase on fundamental natural frequency can also be seen from these figures. This is because of slight thickness increment of the beam at the location of the damage which causes a local increase in bending stiffness.

From Fig. 12, it is seen that the variation of second natural frequency of beams with impact energy induced on them shows generally an irregular trend. The biggest decrease in 2^{nd} natural frequency, which is around 7%, is seen in beam configuration of CG0.

From Fig. 13 it seen that, similar to fundamental frequency, the 3^{rd} natural frequency is also affected mostly with the usage of mold with span length 40 mm in impact testing. 3^{rd} natural frequency affected least with the usage of SP80 beam type in impact testing. By visualization of Figs. 11-13, it can also be seen that the most effected natural frequency is the 2^{nd} one for all beams types and configurations with the increase of impact energy induced on them.

4.3 Buckling behaviors of composites

After the impact and vibration tests, to determine the buckling behavior of the composite specimens, buckling experiments on the specimens impacted at the different span length, orientation angle and energy levels are conducted and the results obtained are given in Fig. 14. The following formal normalized variable is used for critical buckling loads (Eq. (2))

$$P_{cr}^{\ *} = \frac{(P_{cr})_{impacted\_beam}}{(P_{cr})_{intact\_beam}} \tag{2}$$

As can be seen in the figure, $P_{cr}^{\ *}=1$, which is the ratio of the buckling load obtained from the non-impacted specimen itself, is a reference value for normalized critical buckling loads. All tests

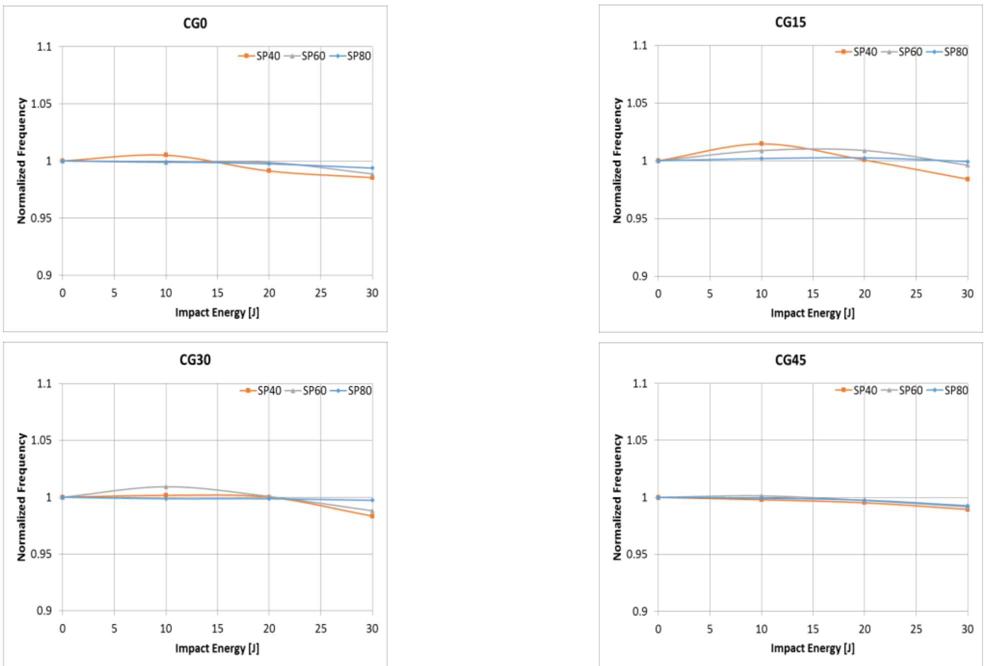

Fig. 13 Variation of third natural frequency of beams with impact energy induced on them

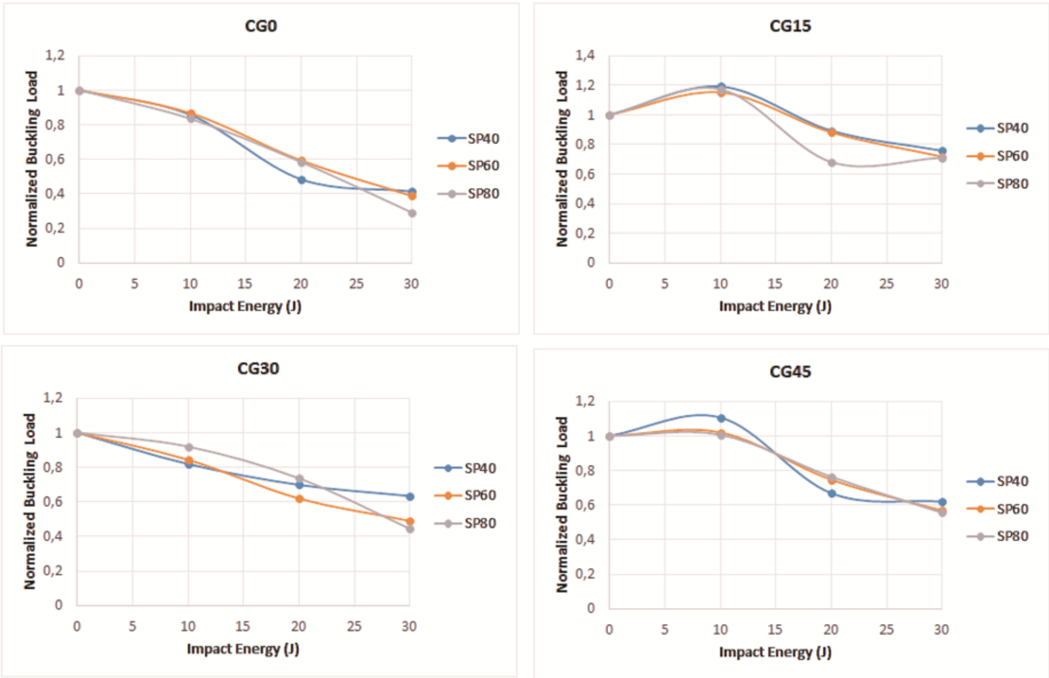

Fig. 14 The variation of the normalized critical buckling loads with increasing impact energy

are conducted for Clamped-Clamped boundary conditions according to uniaxial loading.

In Fig. 14, the distributions of the critical buckling loads versus impact energy levels are drawn for the different orientation angles (0°, 15°, 30° and 45°) and span lengths (40, 60 and 80 mm). The normalized critical buckling loads decrease gradually for CG0 and CG30 configurations as the impact energy increases, but for the other configurations, the critical buckling loads fluctuates as the impact energy increases. For CG15 and CG45 configurations, at low energy levels (up to 10 J), there is an increase in critical buckling loads. As the energy level increases, buckling loads decrease except for CG15 configuration with SP80 beam type.

The loss of the buckling loads for the specimens of CG0 configuration is approximately 62%, CG15, CG30, CG45 are approximately 23%, 50% and 41%, respectively, as taken average values of the all SP types.

4.4 Effect of impact damage on free vibration and buckling

During the impact test, the largest damages are seen on the SP40 beams under 30 J and the damage figures are given in Fig. 15 for these configurations at different orientation angles. The damage areas on the impact side of them are measured as 109, 276, 192, 128 mm^2 for CG0, CG15, CG30, CG45 configurations, respectively, by using SOLIDWORK® commercial program.

For the beams that have 0° orientation angle, the fiber breakages are seen in transverse direction, whereas for the beams that have 15, 30 and 45° orientation angles, both fiber breakages with diamond shape in the transverse direction and indentation in thickness direction are seen. The least diamond shape fiber breakage in the middle zone is seen for CG45 configuration. So, the natural frequency decreases at CG45 configuration are less than CG15 and CG30 configurations,

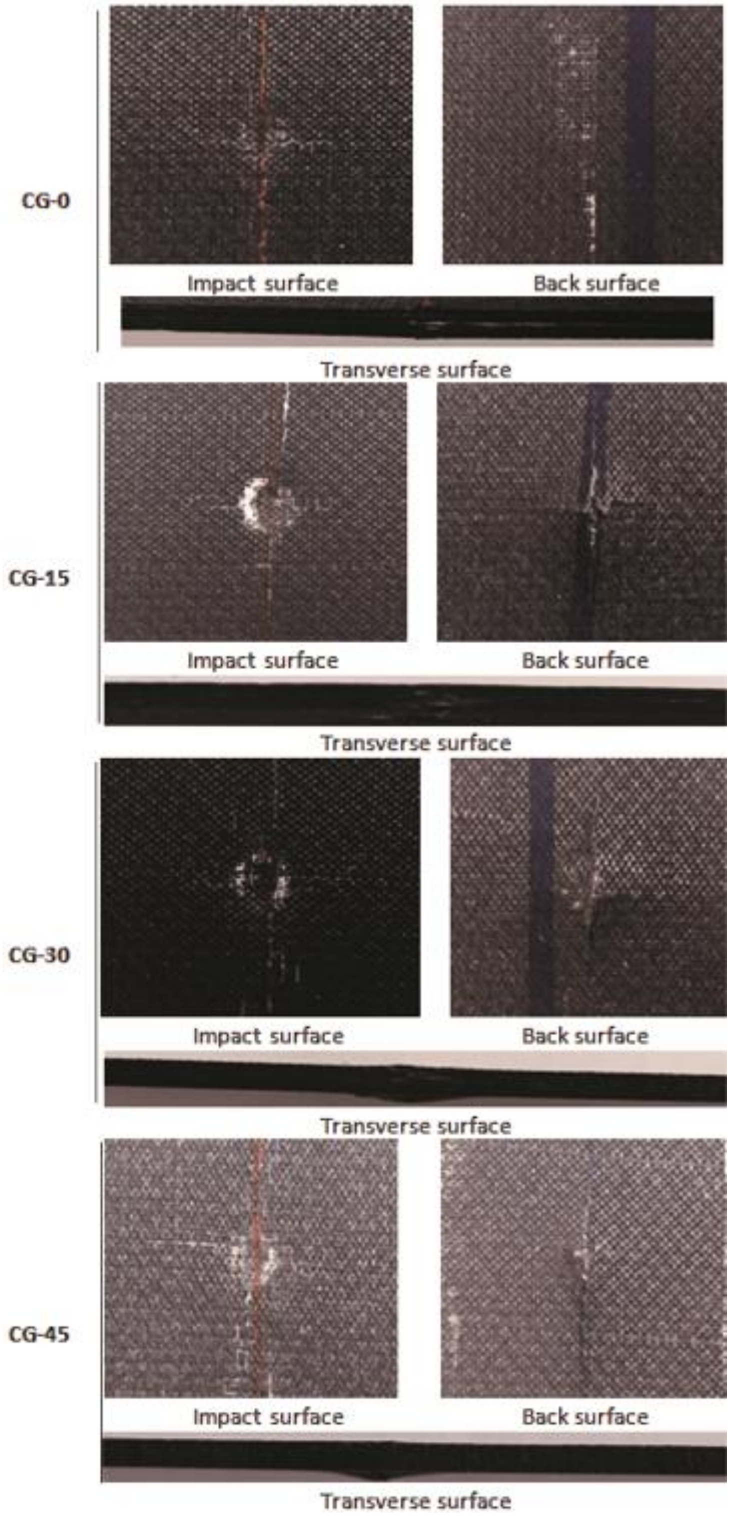

Fig. 15 The damages on the SP40 beams under 30 J for different orientation angles

for the 1^{st} and 3^{rd} modes. For CG0 configuration, there is no diamond shape but only fiber breakages thought the transverse direction are seen which causes local thickness increase in this region, as can be seen from Fig. 15. Because of this reason, the natural frequency for the 1^{st} mode increases for CG0 configuration and the decrease of 3^{rd} natural frequency is less than the configurations with other orientation angles. It can be seen that these changes in the natural frequency vary proportionally by the size of the damaged areas.

For SP40 beams subjected to 30 J impact energy, the biggest decrease as compared to critical buckling load of intact beam is seen for 0° orientation angle which is approximately 60% due to the transverse fiber breakages in the back side. The least decrease, 22%, is seen for CG15 beam configuration due to not expand damage in the back side. The decreases in buckling loads are nearly the same for CG30 and CG45 configurations, which is approximately 38%.

For CG0 configuration, as mentioned before, the complete crack is seen through the transverse direction, which affects critical buckling loads mostly. Also, CG15 and CG45 configurations look graphically similar to each other. The reason of the increase in the critical buckling loads of these configurations under the lower impact energies is the existence of the delamination between the laminates. These variations are similar to the variations of the compression, bending or tensile strengths of the impacted composite beams in literature (Zor *et al*. 2004, Ergun 2010).

5. Conclusions

The free vibration and buckling behaviors of the hybrid composite beams impacted at different energy levels are experimentally analyzed. Impact responses of the hybrid composite specimens are determined first, and then the free vibration and buckling tests are performed on the impacted and intact beams in order to see the effect of the orientation angles and span lengths on natural frequencies and critical buckling loads of the hybrid beams. During the tests, the boundary conditions in ends of the hybrid composite beams are taken clamped-free for free vibration test and clamped-clamped for buckling test. The following results are obtained:

1. Although the hybrid composite beams with the same span length but different orientation angles have the same slope, which represents bending stiffness, their bending stiffness decreases by the increase in the span length
2. It is seen that fundamental natural frequencies of all beams with different configurations are affected mostly by using the mold of the little span length in impact testing.
3. The first and second natural frequencies are the mostly affected ones with the increase in the impact energy.
4. As the normalized critical buckling loads of CG15 and CG45 configurations are increased at the lower energy levels, they are dramatically decreased at the other energy levels and the orientation angles.
5. The critical buckling loads of CG0 configuration are mostly affected as the energy level increases because of the complete crack seen through the transverse direction.
6. The largest damage is seen on the SP40 beams under 30 J for all configurations.
7. The decrease in the natural frequency of CG45 configuration is less than CG15 and CG30 configurations, for the 1^{st} and 3^{rd} modes. Namely, it is shown that the decrease in the natural frequencies vary in proportion with the damage size.
8. Due to the local thickness increase, the natural frequency of CG0 configuration increases for the 1^{st} mode.

References

Çallioğlu, H. and Ergun E. (2014), "Buckling behaviors of the impacted composite plates", *Sci. Eng. Compos. Mater.*, **21**(3), 463-470.

Davoodi, M.M., Sapuan, S.M., Ahmad, D., Aidy, A., Khalina, A. and Jonoobi, M. (2012), "Effect of polybutylene terephthalate (PBT) on impact property improvement of hybrid kenaf/glass epoxy composite", *Mater. Lett.*, **67**(1), 5-7.

Ergun, E. (2010), "Experimental and numerical buckling analyses of laminated composite plates under temperature effects", *Adv. Compos. Lett.*, **19**(4), 131-139.

Fiore, V., Di, Bella, G. and Valenza, A. (2011), "Glass-basalt/epoxy hybrid composites for marine applications", *Mater. Des.*, **32**, 2091-2099.

Frieden, J., Cugnoni, J., Botsis, J. and Gmür, T. (2011), "Vibration-based characterization of impact induced delamination in composite plates using embedded FBG sensors and numerical modeling", *Compos. Part B*, **42**, 607-613.

Ghasemnejad, H., Argentiero, Y. and Tez, T.A. (2013), "Barrington PE. Impact damage response of natural stitched single lap-joint in composite structures", *Mater. Des.*, **51**, 552-560.

Gideon, R.K., Zhang, F., Wu, L.W., Sun, B. and Gu, B. (2015), "Damage behaviors of woven basalt-unsaturated polyester laminates under low-velocity impact", *J. Compos. Mater.*, **49**(17), 2103-2118.

Gustin, J., Joneson, A., Mahinfalah, M. and Stone, J. (2005), "Low velocity impact of combination Kevlar/carbon fiber sandwich composites", *Compos Struct.*, **69**(4), 396-406.

Kıral, Z., Içten, B.M. and Kıral, B.G. (2012), "Effect of impact failure on the damping characteristics of beam-like composite structures", *Compos. Part B*, **43**, 3053-3060.

Mishra, S., Mohanty, A.K., Drzal, L.T., Misra, M., Parija, S., Nayak, S.K. and Tripathy, S.S. (2003), "Studies on mechanical performance of bio-fiber/glass reinforced polyester hybrid composites", *Compos. Sci. Tech.*, **63**, 1377-1385.

Naik, N.K., Borade, S.V., Arya, H., Sailendra, M. and Prabhu, S.V. (2002), "Experimental studies on impact behaviour of woven fabric composites: Effect of impact parameters", *J. Reinf. Plast. Compos.*, **21**(15), 1347-1362.

Onal, L. and Adanur, S. (2002), "Effect of stacking sequence on the mechanical properties of glass-carbon hybrid composites before and after impact", *J. Ind. Text.*, **31**(4), 255-271.

Pandya, K.S., Veerraju, C. and Naik, N.K. (2011), "Hybrid composites made of carbon and glass woven fabrics under quasi-static loading", *Mater. Des.*, **32**(7), 4094-4099.

Petrucci, R., Santulli, C., Puglia, D., Nisini, E., Sarasini, F., Tirillò, J., Torre, L., Minak, G. and Kenny, J.M. (2015), "Impact and post-impact damage characterisation of hybrid composite laminates based on basalt fibres in combination with flax, hemp and glass fibres manufactured by vacuum infusion", *Compos. Part B*, **69**, 507-515.

Saeed, M.U., Chen, Z.F., Chen, Z.H. and Li, B.B. (2014), "Compression behavior of laminated composites subjected to damage induced by low velocity impact and drilling", *Compos. Part B*, **56**, 815-820.

Sayer, M., Bektaş, N.B. and Çallioğlu, H. (2010), "Impact behavior of hybrid composite plates", *J. Appl. Poly. Sci.*, **118**, 580-587.

Sevkat, E., Liaw, B., Delale, F. and Raju, B.B. (2010), "Effect of repeated impacts on the response of plain woven hybrid composites". *Compos. Part B*, **41**(5), 403-413.

Siddeswarappa, B. and Mohamed, K.K. (2009), "Damage characteristics of fabric reinforced hybrid composite laminates subjected to low energy impacts", *Int. J. Mater. Prod. Tech.*, **34**, 303-311.

Swolfs, Y., Gorbatikh, L. and Verpoest, I. (2013), "Stress concentrations in hybrid unidirectional fiber reinforced composites with random fiber packings", *Compos. Sci .Technol.*, **85**, 10-16.

Tercan, M. and Aktas, M. (2009), "Buckling behavior of 1×1 rib knitting laminated plates with cutouts", *Compos. Struct.*, **89**, 245-252.

Velmurugan, R. and Balaganesan, G. (2011), "Modal analysis of pre and post impacted nano composite laminates", *Lat. Am. J. Solid. Struct.*, **8**, 9-26.

Wu, Z.S., Wang, X., Iwashita, K., Sasaki, T. and Hamaguchi, Y. (2010), "Tensile fatigue behavior of FRP and hybrid FRP sheets", *Compos. Part B*, **41**(5), 396-402.

Zor, M., Callioglu, H. and Akbulut, H. (2004), "Three-dimensional buckling analysis of thermoplastic composite laminated plates with single vertical or horizontal strip delamination", *J. Therm. Compos. Mater.*, **17**, 557-568.

CC